

Asteroseismic Diagnostics for Semi-Convection in B Stars in the Era of K2

Ehsan Moravveji¹ †

¹Instituut voor Sterrenkunde, KU Leuven, Celestijnenlaan 200D, B-3001 Leuven, Belgium
email: Ehsan.Moravveji@ster.kuleuven.be

Abstract. Semi-convection is a slow mixing process in chemically-inhomogeneous radiative interiors of stars. In massive OB stars, it is important during the main sequence. However, the efficiency of this mixing mechanism is not properly gauged yet. Here, we argue that asteroseismology of β Cep pulsators is capable of distinguishing between models of varying semi-convection efficiencies. We address this in the light of upcoming high-precision space photometry to be obtained with the *Kepler* two-wheel mission for massive stars along the ecliptic.

Keywords. asteroseismology, stars: oscillations (including pulsations), stars: interiors, stars: evolution, stars: rotation, variables: others

1. Introduction

Non-radial pulsation is a common phenomenon among B dwarfs. Early-type B stars - widely known as β Cep stars - are pulsationally unstable against low-order, low-degree radial and non-radial pressure (p-) and gravity (g-) modes. Their mass ranges from ~ 8 to $20 M_{\odot}$ (see Aerts et al. 2010, for details). Contrary to their fully mixed convective cores, the mixing of species in their radiative interior occurs on a long - yet unconstrained - time scale. There are several mixing mechanisms that operate (simultaneously) in radiative zones, among which rotational mixing and semi-convection. In this paper, we limit ourselves to slowly-rotating B stars.

The pulsation frequencies of stars are highly sensitive to their internal structure, and can be used as a proxy to test different input physics. Miglio et al. (2008) already showed the effect of extra mixing induced by, e.g., rotation, atomic diffusion, and convective overshooting on the period spacing of g-modes in heat-driven pulsators; their conclusions can be extended to include semi-convection as an extra mixing mechanism.

In the near future, the *Kepler* two-wheel mission, (hereafter K2, Howell et al. 2014) will provide high-precision space photometry of a handful of late-O and early B-type pulsators in the ecliptic plane. We emphasise that K2 will conduct pioneering observations, since such space photometry is scarce for massive stars, particularly for objects more massive than $8 M_{\odot}$.

In this paper, we put forward asteroseismic diagnostics to probe semi-convective mixing in massive main-sequence stars. Following on Miglio et al. (2008), we address the possibility of constraining the efficiency of semi-convection in massive stars in light of the upcoming high-precision data to be assembled by the K2 mission and already present in the CoRoT archive.

† Postdoctoral Fellow of the Belgian Science Policy Office (BELSPO), Belgium

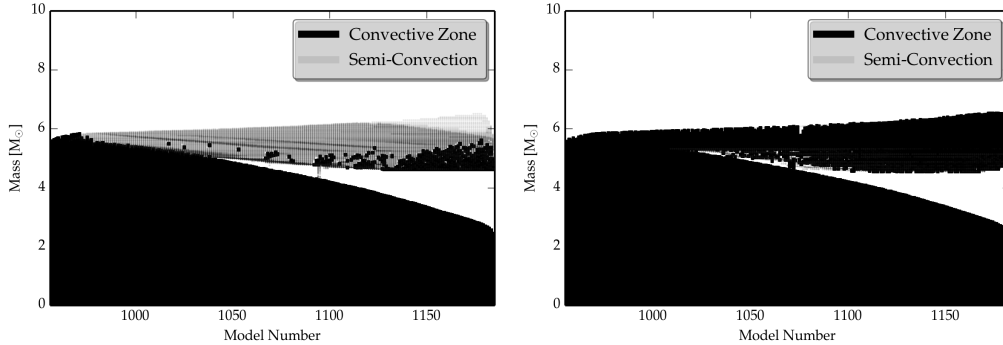


Figure 1. Kippenhahn diagrams showing the evolution of $15 M_{\odot}$ stellar models with $\alpha_{sc} = 10^{-1}$ (left) and $\alpha_{sc} = 1$ (right). The convective zones are shown in blue, and the semi-convective zones are shown in purple.

2. Semi-Convective Mixing

Semi-convection is a slow mixing process believed to operate in the chemically inhomogeneous parts of radiative zones, where the g-modes are oscillatory (Schwarzschild & Härm 1958; Kato 1966; Langer et al. 1983; Noels et al. 2010). In other words, semi-convection acts in those layers of the star where the radiative temperature gradient ∇_{rad} takes values in between the adiabatic ∇_{ad} and the Ledoux ∇_{L} gradients, i.e., $\nabla_{\text{ad}} < \nabla_{\text{rad}} < \nabla_{\text{L}}$. Here, $\nabla_{\text{L}} = \nabla_{\text{ad}} + \varphi/\delta \nabla_{\mu}$, with $\varphi = (\partial \ln \rho / \partial \ln T)_{P,\mu}$, $\delta = (\partial \ln \rho / \partial \ln \mu)_{P,T}$ and $\nabla_{\mu} = d \ln \mu / d \ln P$. Semi-convection occurs due to the stabilizing effect of the composition gradient ∇_{μ} against the onset of convection in the chemically inhomogeneous layers on top of the receding convective core. This mixing process is believed to be present in stars with $M \gtrsim 15 M_{\odot}$ (Langer et al. 1985; Langer 1991). The reason is the increasing effect of the radiation pressure with mass, and the local increase of ∇_{rad} with respect to ∇_{ad} outside the convective core. Therefore, semi-convection is not expected in intermediate to late B-type stars. For this reason, β Cep stars are optimal candidates to investigate if such a mixing can leave observable footprints. The semi-convective mixing is typically described in a diffusion approximation (Langer et al. 1983). See Section 6.2 in Maeder (2009) for an overview of different mixing schemes.

The stellar evolution code MESA (Paxton et al. 2011, 2013) follows the prescription by Langer et al. (1985), where the semi-convective diffusion coefficient D_{sc} is defined according to Kato (1966) and Langer et al. (1983):

$$D_{\text{sc}} = \alpha_{\text{sc}} \frac{\kappa_r}{6c_p \rho} \frac{\nabla - \nabla_{\text{ad}}}{\nabla_{\text{L}} - \nabla}, \quad (2.1)$$

where $\kappa_r = 4acT^3/3\kappa\rho$ is the radiative conductivity, c_p the specific heat at constant pressure, and ρ denotes the density. The efficiency of semi-convective mixing is controlled by the free parameter α_{sc} , which determines the length scale and time scale of the vibrational mixing associated to semi-convective zones. The parameter α_{sc} is not calibrated from observations, Langer et al. (e.g., 1985) favoured $\alpha_{\text{sc}} = 10^{-1}$, while later on Langer (1991) preferred $0.01 \leq \alpha_{\text{sc}} \leq 0.04$. Note that the value of α_{sc} depends on the choice of the opacity tables and on the numerical scheme to compute D_{sc} according to Eq. (2.1). We aim at constraining α_{sc} using K2 data.

3. Effect of Semi-Convection on β Cep models

We used the MESA code to calculate four evolutionary tracks for a $15 M_{\odot}$ star with initial chemical composition $(X, Y, Z) = (0.710, 0.276, 0.014)$ based on Nieva & Przybilla (2012). We excluded mass loss in all models and considered four values of $\alpha_{\text{sc}} = 10^{-6}$, 10^{-4} , 10^{-2} , and 1. We used the Ledoux criterion of convection, and made sure that the condition $\nabla_{\text{rad}} = \nabla_{\text{ad}} = \nabla_{\text{L}}$ was satisfied from the convective side of the core boundary (Gabriel et al. 2014); see also Noels (these proceedings). On each evolutionary track, we stored an equilibrium model for a central hydrogen abundance of $X_c = 0.10$. We subsequently used the GYRE pulsation code (Townsend & Teitler 2013) to calculate radial $\ell = 0$, dipole $\ell = 1$ and quadrupole $\ell = 2$ mode frequencies in the adiabatic approximation, for each model. We restricted the comparison of the mode behaviour to low-order modes, i.e., $-5 \leq n_{\text{pg}} \leq +3$, where $n_{\text{pg}} = n_{\text{p}} - n_{\text{g}}$.

Figure 1 shows Kippenhahn diagrams for models with $\alpha_{\text{sc}} = 10^{-2}$ (left) and $\alpha_{\text{sc}} = 1$ (right). For relatively limited semi-convective mixing (i.e., $\alpha_{\text{sc}} = 10^{-2}$), an extended semi-convective zone (grey points) develops and continues at roughly the same mass coordinate. On the other hand, for efficient semi-convective mixing (i.e. $\alpha_{\text{sc}} = 1$) the former zones are identified as convective and an extended intermediate convective zone (hereafter ICZ) develops. In our models, the ICZ encapsulates $\sim 1 M_{\odot}$. The formation and presence of an ICZ largely impacts the later evolution of the star. From an asteroseismic point of view, models harbouring an ICZ have smaller radiative zones (measured from the surface), hence a smaller cavity for g-mode propagation. As a result, it is expected that the presence of an ICZ, which in turn results from different semi-convective efficiencies, affects the adiabatic frequencies of low-order low-degree p- and g-modes.

A word of caution about matching detected frequencies of unidentified modes from a grid of asteroseismic models is worthwhile to be made here. Figure 2a shows that the frequency of the radial fundamental mode $\ell = 0, n_{\text{pg}} = 1$ is quite close to that of an $\ell = 2, n_{\text{pg}} = -2$ non-radial g-mode. Without robust mode identification — which by itself is intricate — the interpretation of detected pulsation frequencies can be quite misleading. Therefore, the photometric light curves to be assembled by K2 must be complemented with ground-based multi-colour photometry and/or high-resolution spectroscopy to identify at least one of the detected modes. Non-adiabatic computations might help to identify modes, although there are still severe disagreements between the observed modes in OB stars and those predicted to be excited in the sense that we detect many more modes than foreseen by theory. It is therefore safer not to rely on excitation computations when identifying detected frequencies.

Figure 2a shows the frequencies of $\ell = 0, 1$ and 2 p- and g-modes for different values of α_{sc} . For better visibility, few modes with identical ℓ and n_{pg} are connected by lines. Clearly, the change in α_{sc} shifts most of the frequencies to slightly lower/higher values. The frequency difference of the modes with fixed ℓ and n_{pg} increases with decreasing α_{sc} . An important question is whether we are able to capture such subtle differences observationally from the K2 space photometry.

To answer that, we take the model with $\alpha_{\text{sc}} = 1$ as the *reference* model, hence its frequencies are $f_i^{(\text{ref})}$. We compare the relative frequency change $\delta f_i^{(\text{th})}$ of each theoretical frequency f_i with respect to the reference frequency as

$$\delta f_i^{(\text{th})} = \frac{|f_i^{(\text{ref})} - f_i|}{f_i^{(\text{ref})}}. \quad (3.1)$$

Here, $f_i^{(\text{ref})}$ and f_i are both calculated using GYRE. From an observational point of view, the frequency precision Δf depends on the total observation time base ΔT . A

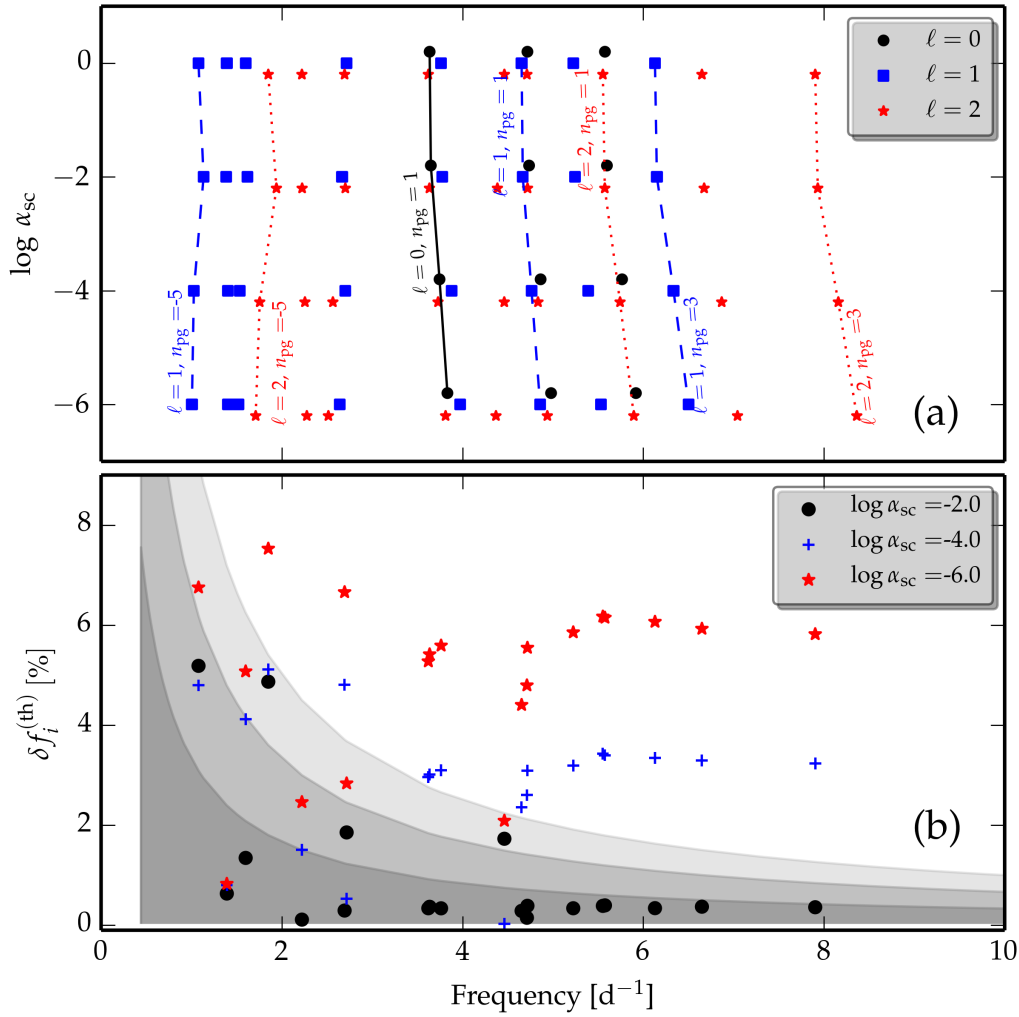


Figure 2. Adiabatic low radial order $-5 \leq n_{\text{pg}} \leq +3$ frequencies of $15 M_{\odot}$ models with $Z=Z_{\odot}$ and $X_c = 0.10$. Both panels share the same frequency range on the abscissa. (a) The ordinate is the logarithm of α_{sc} (Eq. 2.1). Circles are radial $\ell = 0$ modes, squares are non-radial dipole $\ell = 1$ p- and g-modes, and stars are non-radial quadrupole $\ell = 2$ p- and g-modes. (b) Comparison of the relative theoretical frequency change $\delta f_i^{(\text{th})}$ with the relative observed frequency precision $\delta f_i^{(\text{obs})}$ as a function of frequency; see Eqs. (3.1) and (3.2). Dark grey, grey and light grey show 1σ , 2σ and 3σ precision levels, respectively. Circles, plus marks, and stars correspond to models with $\alpha_{\text{sc}} = 10^{-2}$, 10^{-4} , and 10^{-6} , respectively. The reference frequencies are taken from the $\alpha_{\text{sc}} = 1$ model. Consult the color version of this figure in electronic format.

conservative estimate by Loumos & Deeming (1978) is $\Delta f \approx 2.5/\Delta T$. For K2, the planned ΔT is approximately 75 days. We also define the relative observed frequency precision $\delta f_i^{(\text{obs})}$

$$\delta f_i^{(\text{obs})} = \frac{\Delta f}{f_i^{(\text{ref})}}, \quad (3.2)$$

where $\delta f_i^{(\text{obs})}$ stands for a 1σ uncertainty level, and measures the observational frequency precision required to capture the effect of a specific feature — in our case the

presence/absence of the ICZ. If by varying a stellar structure free parameter — here α_{sc} — the relative theoretical frequency change is significantly larger than the estimated observational relative frequency precision, i.e. $\delta f_i^{(\text{th})} \gtrsim 3 \delta f_i^{(\text{obs})}$, then asteroseismology can constrain the value of that parameter. Note the arbitrary choice of 3σ here.

To visualise the probing power of the K2 data, Figure 2b shows the relative frequency change $\delta f_i^{(\text{th})}$ with respect to the reference model ($\alpha_{\text{sc}} = 1$) for models with $\log \alpha_{\text{sc}} = -2$ (circles), -4 (plus marks) and -6 (stars), respectively. In the background of the same plot, we show $\delta f_i^{(\text{obs})}$ (dark grey), $2 \times \delta f_i^{(\text{obs})}$ (grey) and $3 \times \delta f_i^{(\text{obs})}$ (light grey), respectively. The distribution of the circles is roughly inside the 1σ zone, which makes the distinction between models with $\alpha_{\text{sc}} = 1$ and $\alpha_{\text{sc}} = 10^{-2}$ quite challenging. However, plus marks that compare $\log \alpha_{\text{sc}} = 10^{-4}$ models with those of the reference model, or stars that compare $\log \alpha_{\text{sc}} = 10^{-6}$ models with the reference model are more than 3σ away from $\delta f^{(\text{obs})}$. For the latter, K2 holds the potential to constrain the efficiency of semi-convection as an extra mixing mechanism, provided that we can find good seismic models of the stars according to the scheme outlined in Aerts (these proceedings) to which we then add the concept of semi-convective mixing.

4. Conclusions

Unfortunately, the *Kepler* mission observed no O-type and early-B stars so far. Thus, we are yet unable to estimate the richness of the frequency spectrum of the K2 light curves for massive dwarfs. The public release of the K2 field 0 light curves is scheduled for September 2014; since there are several OB pulsators on K2 silicon, we will soon be able to gauge the quality of K2 data for massive star asteroseismology.

In our comparisons, we assumed that the K2 data do not suffer from instrumental effects, hence that $\delta f^{(\text{obs})}$ depends only on the time base of the K2 campaigns. This is of course an idealised situation. The telescope jitter and drift can easily increase $\delta f^{(\text{obs})}$. Yet, the seismic diagnostic potential stays valid since the $\delta f^{(\text{th})}$ can exceed the 3σ level for several modes, and hence the effect of semi-convective mixing can hopefully be detected and studied using K2 light curves.

Based on Figure 2, there is no real preference between modes of different order n_{pg} and degree ℓ in providing asteroseismic diagnostics for semi-convection; in other words, all low-order p- and g-modes possess the same potential to provide a constraint on α_{sc} . The semi-convection free parameter was varied in a broad range, from 10^{-6} to 1, in our exercise. It is of course easier to discriminate between models with large differences in α_{sc} . According to Figure 2b, the distinction between models with $\alpha_{\text{sc}} = 10^{-6}$ and 1 is more within reach than distinguishing between models with $\alpha_{\text{sc}} = 10^{-2}$ and 1.

The main message of our work is to emphasize the importance of semi-convection along with the shrinking convective cores in massive OB stars, when the observed frequencies of β Cep stars are compared with theoretical frequencies. Consequently, semi-convection — as one of the extra mixing mechanisms in inhomogeneous layers of the stellar radiative interior — could be employed as an extra dimension when modelling stars based on grid calculations coupled to asteroseismic forward modelling (Briquet et al. 2007).

References

- Aerts, C., Christensen-Dalsgaard, J., & Kurtz, D. W. 2010, *Asteroseismology, Astronomy and Astrophysics Library, Springer Berlin Heidelberg*
- Briquet, M., Morel, T., Thoul, A., et al. 2007, *MNRAS* 381, 1482
- Gabriel, M., Noels, A., Montalbán, J., & Miglio, A. 2014, *ArXiv e-prints*

- Howell, S. B., Sobek, C., Haas, M., et al. 2014, *PASP* 126, 398
- Kato, S. 1966, *PASJ* 18, 374
- Langer, N. 1991, *A&A* 252, 669
- Langer, N., El Eid, M. F., & Fricke, K. J. 1985, *A&A* 145, 179
- Langer, N., Fricke, K. J., & Sugimoto, D. 1983, *A&A* 126, 207
- Loumos, G. L. & Deeming, T. J. 1978, *Ap&SS* 56, 285
- Maeder, A. 2009, *Physics, Formation and Evolution of Rotating Stars*
- Miglio, A., Montalbán, J., Noels, A., & Eggenberger, P. 2008, *MNRAS* 386, 1487
- Mowlavi, N. & Forestini, M. 1994, *A&A* 282, 843
- Nieva, M.-F. & Przybilla, N. 2012, *A&A* 539, A143
- Noels, A., Montalbán, J., Miglio, A., Godart, M., & Ventura, P. 2010, *Ap&SS* 328, 227
- Pápics, P. I., Moravveji, E., Aerts, C., et al. 2014, *A&A*, in press (arXiv1407.2986)
- Paxton, B., Bildsten, L., Dotter, A., et al. 2011, *ApJS* 192, 3
- Paxton, B., Cantiello, M., Arras, P., et al. 2013, *ApJS* 208, 4
- Schwarzschild, M. & Härm, R. 1958, *ApJ* 128, 348
- Townsend, R. H. D. & Teitler, S. A. 2013, *MNRAS* 435, 3406